

Article

Computer Modelling of Hafnium Doping in Lithium Niobate

Romel M. Araujo ¹, Mario E. G. Valerio ²  and Robert A. Jackson ^{3,*} 

¹ Chemistry Coordination/IPISE/PIC, Pio Decimo College, Campus III, Aracaju-SE 49027-210, Brazil; raraujoster@gmail.com

² Physics Department, Federal University of Sergipe, Campus Universitário, São Cristovão-SE 491000-000, Brazil; megvalerio@gmail.com

³ Lennard-Jones Laboratories, School of Chemical and Physical Sciences, Keele University, Keele, Staffordshire ST5 5BG, UK

* Correspondence: r.a.jackson@keele.ac.uk

Received: 3 January 2018; Accepted: 1 March 2018; Published: 6 March 2018

Abstract: Lithium niobate (LiNbO₃) is an important technological material with good electro-optic, acousto-optic, elasto-optic, piezoelectric and nonlinear properties. Doping LiNbO₃ with hafnium (Hf) has been shown to improve the resistance of the material to optical damage. Computer modelling provides a useful means of determining the properties of doped and undoped LiNbO₃, including its defect chemistry, and the effect of doping on the structure. In this paper, Hf-doped LiNbO₃ has been modelled, and the final defect configurations are found to be consistent with experimental results.

Keywords: lithium niobate; hafnium doping; computer modelling

1. Introduction

Lithium niobate (LiNbO₃) is a material with many important technological applications that result from its diverse physical properties [1–4]. Laser-induced optical damage or so-called photorefractive damage was first observed in LiNbO₃ and LiTiO₃ crystals at the Bell Laboratories [5]. This effect can be utilized for holographic information storage and optical amplification; however, it hinders the usage of LiNbO₃ in frequency doublers, Q-switchers and optical waveguides, so ways of minimising this optical damage have been sought actively. Kokanyan et al. [6] reported that the light-induced birefringence changes of LiNbO₃ crystals doped with 4 mol % of HfO₂ were comparable to that of 6 mol % MgO doped crystals, indicating that Hf doping is effective in resisting optical damage.

Much useful information about lithium niobate and its defect properties can be obtained by computer modelling, based on the description of interactions between ions by effective potentials. Previous papers have reported the derivation of an interatomic potential for LiNbO₃ [7], the doping of the structure by rare earth ions [8,9], doping with Sc, Cr, Fe and In [10], and metal co-doping [11]. These papers show that modelling can predict the energetically optimal locations of the dopant ions, and calculate the energy involved in the doping process, making it a suitable method to study Hf-doped lithium niobate, with the aim of establishing the optimal doping site and charge compensation scheme.

2. Methodology

In this paper, use is made of the lattice energy minimisation method, in which the lattice energy of a given structure is calculated, and the structure varied until a minimum in the energy is found. This approach has been applied to a wide range of inorganic materials, with specific applications to LiNbO₃ reported in references [7–11]. The method makes use of interatomic potentials to describe the interactions between ions in the solid, as described in the next Section 2.1. Defects in solids are

modelled using the Mott-Littleton method [12] which is described in Section 2.2. All calculations were performed using the GULP code [13].

2.1. Interatomic Potentials

In this paper use has been made of a previously derived potential for LiNbO₃ [7], and a potential fitted to the structure of HfO₂. In both cases, a Buckingham potential is employed, supplemented by an electrostatic interaction term:

$$V = \frac{q_1 q_2}{r} + A \exp\left(\frac{-r}{\rho}\right) - Cr^{-6}$$

In this potential, q_1 and q_2 are the charges on the interacting ions separated by a distance r , and A , ρ and C are parameters that are fitted empirically.

The derivation of potentials for LiNbO₃ and HfO₂ are considered separately below.

2.1.1. LiNbO₃

Full details of the derivation of the LiNbO₃ potential are given in reference [7], but they will be summarised here. The potential was derived empirically by simultaneously fitting to the structures of LiNbO₃, Li₂O and Nb₂O₅. The O²⁻-O²⁻ potential obtained by Catlow [14] was retained as this is widely used in many other oxides. The O²⁻ ion was described using the shell model [15], and a 3 body potential was used to model the interactions between niobium ions and nearest oxygen neighbours, which takes the form:

$$V_{3\text{ body}} = 1/2 k (\theta - \theta_0)^2$$

In this equation θ_0 is the equilibrium bond angle and k_θ is the bond-bending force constant. The potential parameters are given in Table 1 below:

Table 1. Potential parameters for LiNbO₃ [7].

Interaction	A (eV)	ρ (Å)	C (eV Å ⁶)
Nb _{core} -O _{shell}	1425.0	0.3650	0.0
Li _{core} -O _{shell}	950.0	0.2610	0.0
O _{shell} -O _{shell}	22,764.0	0.1490	27.88
Shell Parameters	Shell Charge, Y (e)	Spring Constant, k_r (eV Å ⁻²)	
O ²⁻	-2.9	70.0	
3 body Parameters	Force Constant, k_θ (eV rad ⁻²)	Equilibrium Angle, θ_0	
O _{shell} -Nb _{core} -O _{shell}	0.5776	90.0	

A comparison of experimental [16] and calculated lattice parameters of LiNbO₃ can be found in Table 2, showing that the derived potential reproduces the structural parameters to within a few percent.

Table 2. Comparison of experimental [16] and calculated lattice parameters for LiNbO₃.

Parameter	Experimental	Calculated (0 K)	$\Delta\%$	Calculated (295 K)	$\Delta\%$
a = b (Å)	5.1474	5.1559	0.17	5.1868	0.77
c (Å)	13.8561	13.6834	1.24	13.7103	1.05

2.1.2. HfO₂

A potential was derived for HfO₂ by fitting to its structure [17]. The potential parameters are given in Table 3 (with the O²⁻ shell parameters having the same values as in LiNbO₃), and the agreement

between calculated and experimental lattice parameters calculated at 0 K and 293 K is shown in Table 4. As is seen from the $\Delta\%$ values, good agreement is obtained using this potential.

Table 3. Interionic potentials obtained from a fit to the HfO₂ structure [17].

Interaction	A (eV)	ρ (Å)	C (eV Å ⁶)
Hf _{core} –O _{shell}	1413.54	0.3509	0.0
O _{shell} –O _{shell}	22764.0	0.1490	27.88

Table 4. Comparison of calculated and experimental lattice parameters.

Parameter	Experimental [17]	Calculated (0 K)	$\Delta\%$	Calculated (295 K)	$\Delta\%$
a = b = c (Å)	5.084000	5.084236	0.00	5.087119	0.06

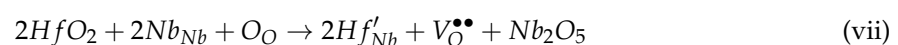
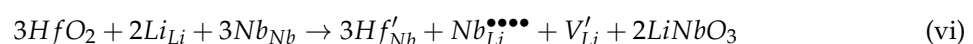
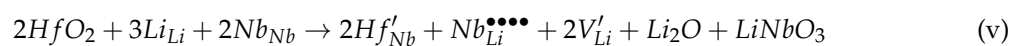
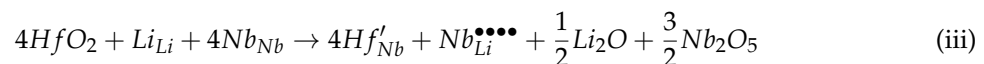
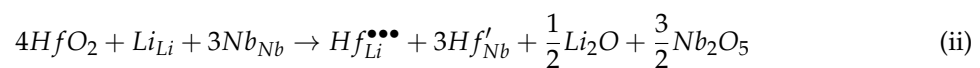
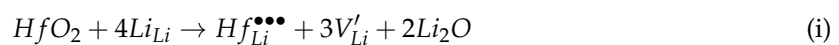
2.2. Defect Calculations

The calculations are carried out using the Mott–Littleton method [12], in which point defects are considered to be at the centre of a region in which all interactions are treated explicitly, while approximate methods are employed for regions of the lattice more distant from the defect. In practice, this involves placing the Hf⁴⁺ ion at either the Li⁺ or Nb⁵⁺ site, along with a range of charge compensating defects, as listed below, using schemes (i) and (ii) suggested by Li et al. [18], plus a further 5 schemes ((iii)–(vii)) proposed here:

- (i) An Hf⁴⁺ ion at a Li⁺ site, with charge compensation by 3 Li⁺ vacancies
- (ii) An Hf⁴⁺ ion at a Li⁺ site, with charge compensation by 3 Hf⁴⁺ ions at Nb⁵⁺ sites
- (iii) 4 Hf⁴⁺ ions at Nb⁵⁺ sites, with charge compensation by a Nb⁵⁺ ion at a Li⁺ site
- (iv) An Hf⁴⁺ ion at a Nb⁵⁺ site, with charge compensation by a Nb⁵⁺ ion at a Li⁺ site and 3 Li⁺ vacancies
- (v) 2 Hf⁴⁺ ions at Nb⁵⁺ sites, with charge compensation by a Nb⁵⁺ ion at a Li⁺ site and 2 Li⁺ vacancies
- (vi) 3 Hf⁴⁺ ions at Nb⁵⁺ sites, with charge compensation by a Nb⁵⁺ ion at a Li⁺ site and 1 Li⁺ vacancy
- (vii) 2 Hf⁴⁺ ions at Nb⁵⁺ sites, with charge compensation by an O^{2−} vacancy

3. Results and Discussion

The seven mechanisms described in Section 2.2 have been written below as solid-state reactions, employing Kroger–Vink notation [19]:



The energies corresponding to these reactions are defined as solution energies, E_s , and they are calculated as follows:

$$E_s = E(\text{Hf}_{\text{Li}}^{\bullet\bullet\bullet} + 3V'_{\text{Li}}) + 2E_{\text{latt}}(\text{Li}_2\text{O}) - E_{\text{latt}}(\text{HfO}_2) \quad (\text{i})$$

$$E_s = E(Hf_{Li}^{\bullet\bullet\bullet} + 3Hf'_{Nb}) + \frac{3}{2}E_{latt}(Nb_2O_5) + \frac{1}{2}E_{latt}(Li_2O) - 4E_{latt}(HfO_2) \quad (ii)$$

$$E_s = E(4Hf'_{Nb} + Nb_{Li}^{\bullet\bullet\bullet\bullet}) + \frac{3}{2}E_{latt}(Nb_2O_5) + \frac{1}{2}E_{latt}(Li_2O) - 4E_{latt}(HfO_2) \quad (iii)$$

$$E_s = E(Hf'_{Nb} + Nb_{Li}^{\bullet\bullet\bullet\bullet} + 3V'_{Li}) + 2E_{latt}(Li_2O) - E_{latt}(HfO_2) \quad (iv)$$

$$E_s = E(2Hf'_{Nb} + Nb_{Li}^{\bullet\bullet\bullet\bullet} + 2V'_{Li}) + E_{latt}(Li_2O) + E_{latt}(LiNbO_3) - 2E_{latt}(HfO_2) \quad (v)$$

$$E_s = E(3Hf'_{Nb} + Nb_{Li}^{\bullet\bullet\bullet\bullet} + V'_{Li}) + 2E_{latt}(LiNbO_3) - 3E_{latt}(HfO_2) \quad (vi)$$

$$E_s = E(2Hf'_{Nb} + V_{O}^{\bullet\bullet}) + E_{latt}(Nb_2O_5) - 2E_{latt}(HfO_2) \quad (vii)$$

Lattice energies, E_{latt} , required to calculate the solution energies, are given in Table 5. Table 6 gives the formation energies of the bound defects (the first term in the above equations). Table 7 gives the solution energy for each scheme (determined using the expressions above), and it is noted that the lowest energy corresponds to scheme (vi), where 3 Hf^{4+} ions substitute at Nb^{5+} sites, with charge compensation by a Nb^{5+} ion at a Li^+ site and 1 Li^+ vacancy, and the second lowest energy scheme is (ii), which involves the Hf^{4+} ion substituting at both cation sites (self-compensation). Experimental data [18,20] supports the self-compensation model, and it is noted that at 293 K the calculated energetic preference for scheme (vi) is only 0.06 eV. However, it is noted that the calculations in this paper have been made at infinite dilution, and experimental data suggests that if dopant concentration is taken into account, Hf in low concentrations occupies the Li^+ site [21–23], and that occupancy of both Li^+ and Nb^{5+} sites only happens once the optical damage threshold is passed [18,23]. Future calculations will be carried out which will model the effect of Hf concentration on the preferred dopant sites, enabling comparison with these results to be made.

Table 5. Lattice energies used in the solution energy calculations (eV).

Structures	0 K	293 K
$LiNbO_3$	−174.57	−174.66
Li_2O	−33.16	−32.92
Nb_2O_5	−314.37	−313.99
HfO_2	−110.39	−110.45

Table 6. Defect formation energies, in eV, for the bound defect.

Defect	Scheme (i)		Scheme (ii)		Scheme (iii)		Scheme (iv)		Scheme (v)		Scheme (vi)		Scheme (vii)	
	0	293	0	293	0	293	0	293	0	293	0	293	0	293
T (K)	0	293	0	293	0	293	0	293	0	293	0	293	0	293
Hf^{4+}	−36.03	−36.35	52.51	52.27	53.34	53.11	−33.85	−34.01	−2.61	−2.73	25.40	25.07	97.82	97.64

Table 7. Solution energies, in eV, for the bound defect (per dopant ion).

Defect	Scheme (i)		Scheme (ii)		Scheme (iii)		Scheme (iv)		Scheme (v)		Scheme (vi)		Scheme (vii)	
	0	293	0	293	0	293	0	293	0	293	0	293	0	293
T (K)	0	293	0	293	0	293	0	293	0	293	0	293	0	293
Hf^{4+}	8.26	8.04	1.65	1.48	1.86	1.69	5.25	5.11	2.12	2.09	1.49	1.42	2.28	2.11

4. Conclusions

This paper has presented a computational study of Hf^{4+} -doped $LiNbO_3$. Solution energies have been calculated for seven possible mechanisms by which the Hf^{4+} might be incorporated in the structure, and the lowest energy scheme, involving self-compensation, is shown to be consistent with some experimental data, although future calculations including Hf concentration will be carried out to investigate this further.

Acknowledgments: The authors are grateful to CAPES and FINEP for financial support.

Author Contributions: Romel M. Araujo carried out the calculations, Mario E. G. Valerio and Robert A. Jackson analysed the results and Robert A. Jackson wrote the paper.

Conflicts of Interest: The authors declare no conflict of interest.

References

1. Jazbinsek, M.; Zgonik, M. Material tensor parameters of LiNbO₃ relevant for electro-and elasto-optics. *Appl. Phys. B* **2002**, *74*, 407.
2. Rauber, A. *Current Topics in Materials Science*; Kaldis, E., Ed.; North-Holland: Amsterdam, The Netherlands, 1978; Volume 1, p. 481.
3. Prokhorov, A.M.; Kuzminov, Y.S. *Physics and Chemistry of Crystalline Lithium Niobate*, 1st ed.; Hilger: New York, NY, USA, 1990.
4. Wong, K.K. (Ed.) *Properties of Lithium Niobate*; IEE: London, UK, 2004.
5. Askin, A.; Boyd, G.D.; Dziedzic, J.M.; Smith, R.G.; Ballman, A.A.; Levinstein, J.J.; Nassau, K. Optically-induced refractive index inhomogeneities in LiNbO₃, and LiTaO₃. *Appl. Phys. Lett.* **1966**, *9*, 72. [[CrossRef](#)]
6. Kokanyan, E.P.; Razzari, L.; Cristiani, I.; Degiorgio, V.; Gruber, J.B. Reduced photorefraction in hafnium-doped single-domain and periodically poled lithium niobate crystals. *Appl. Phys. Lett.* **2004**, *84*, 1880. [[CrossRef](#)]
7. Jackson, R.A.; Valerio, M.E.G. A new interatomic potential for the ferroelectric and paraelectric phases of LiNbO₃. *J. Phys. Condens. Matter* **2005**, *17*, 837. [[CrossRef](#)]
8. Araujo, R.M.; Lengyel, K.; Jackson, R.A.; Valerio, M.E.G.; Kovacs, L. Computer modelling of intrinsic and substitutional defects in LiNbO₃. *Phys. Status Solidi (c)* **2007**, *4*, 1201–1204. [[CrossRef](#)]
9. Araujo, R.M.; Lengyel, K.; Jackson, R.A.; Kovacs, L.; Valerio, M.E.G. A computational study of intrinsic and extrinsic defects in LiNbO₃. *J. Phys. Condens. Matter* **2007**, *19*, 046211. [[CrossRef](#)]
10. Araujo, R.M.; Valerio, M.E.G.; Jackson, R.A. Computer modelling of trivalent metal dopants in lithium niobite. *J. Phys. Condens. Matter* **2008**, *20*, 035201. [[CrossRef](#)]
11. Araujo, R.M.; Valerio, M.E.G.; Jackson, R.A. Computer modelling of hafnium doping in lithium niobite. *Proc. R. Soc. A* **2014**, *470*, 0406. [[CrossRef](#)]
12. Mott, N.F.; Littleton, M.J. Conduction in polar crystals. I. Electrolytic conduction in solid salts. *Trans. Faraday Soc.* **1938**, *34*, 485–499. [[CrossRef](#)]
13. Gale, J.D. GULP: A computer program for the symmetry-adapted simulation of solids. *J. Chem. Soc. Faraday Trans.* **1997**, *93*, 629–637. [[CrossRef](#)]
14. Sanders, M.J.; Leslie, M.; Catlow, C.R.A. Interatomic potentials for SiO₂. *J. Chem. Soc. Chem. Commun.* **1984**, 1271–1273. [[CrossRef](#)]
15. Dick, B.J.; Overhauser, A.W. Theory of the dielectric constants of alkali halide crystals. *Phys. Rev.* **1958**, *112*, 90. [[CrossRef](#)]
16. Abrahams, S.C.; Marsh, P. Defect structure dependence on composition in lithium niobite. *Acta Crystallogr. B* **1986**, *42*, 61–68. [[CrossRef](#)]
17. Liu, Q.J.; Liu, Z.T.; Feng, L.P.; Xu, B. Electronic structure, effective masses, mechanical and thermo-acoustic properties of cubic HfO₂ under pressure. *Phys. Status Solidi B* **2011**, *248*, 950–955. [[CrossRef](#)]
18. Li, S.; Liu, S.; Kong, Y.; Deng, D.; Gao, G.; Li, Y.; Gao, H.; Zhang, L.; Hang, Z.; Chen, S.; et al. The optical damage resistance and absorption spectra of LiNbO₃: Hf crystals. *J. Phys. Condens. Matter* **2006**, *18*, 3527–3534. [[CrossRef](#)]
19. Kröger, F.A.; Vink, H.J. The origin of the fluorescence in self-activated ZnS, CdS, and ZnO. *J. Chem. Phys.* **1954**, *22*, 250. [[CrossRef](#)]
20. Marques, J.G.; Kling, A.; de Jesus, C.M.; Soares, J.C.; da Silva, M.F.; Dieguez, E.; Agulló-Lopez, F. Annealing recovery of neutron irradiated LiNbO₃: Hf single crystals. *Nucl. Instrum. Methods Phys. Res. B* **1998**, *141*, 326–331. [[CrossRef](#)]
21. Rebouta, L.; Soares, J.C.; Da Silva, M.F.; Sanz Garcia, J.A.; Dieguez, E.; Agulló-Lopez, F. Determination of lattice sites for Eu, Hf and Nd IN LiNbO₃ by RBS/channeling experiments. *Nucl. Instrum. Methods Phys. Res. B* **1990**, *50*, 428–430. [[CrossRef](#)]

22. Prieto, C.; Zaldo, C.; Fessler, P.; D'Expert, H.; Sanz Garcia, J.A.; Dieguez, E. Lattice position of Hf and Ta in LiNbO₃: An extended X-ray-absorption fine-structure study. *Phys. Rev. B* **1991**, *43*, 2594–2600. [[CrossRef](#)]
23. Hammoum, R.; Fontana, M.D.; Gilliot, M.; Bourson, P.; Kokanyan, E.P. Site spectroscopy of Hf doping in Hf-doped LiNbO₃ crystals. *Solid State Commun.* **2009**, *149*, 1967–1970. [[CrossRef](#)]



© 2018 by the authors. Licensee MDPI, Basel, Switzerland. This article is an open access article distributed under the terms and conditions of the Creative Commons Attribution (CC BY) license (<http://creativecommons.org/licenses/by/4.0/>).